Supporting Information

High Loading of Iridium Single Atoms in $NiCo_2O_4$ for Enhanced Acidic Oxygen Evolution Reaction

Bilal Zaman[#a], Qiwen Su[#a], Dongxu Jiao[a], Ming Gong[a], Mingming Wang[a], Muhammad Faizan[a], Xiaoqiang Cui*[a]

[a] State Key Laboratory of Automotive Simulation and Control, School of Materials Science and Engineering, and Key Laboratory of Automobile Materials of MOE, Jilin University, Changchun, 130012, China.

[#]These authors contributed equally to this work.

*Corresponding Author: Xiaoqiang Cui;

E-mail: xqcui@jlu.edu.cn (X. Q. Cui);

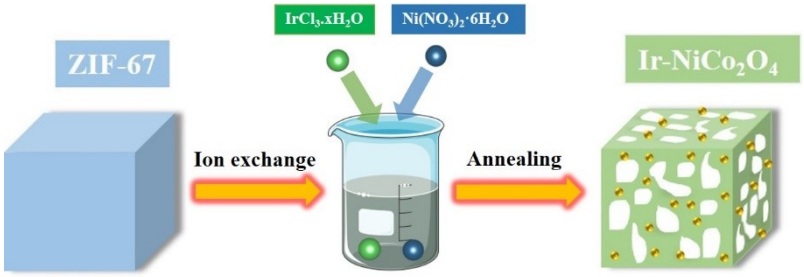

Fig S1. The synthesis procedure of Ir-$NiCo_2O_4$ catalysts.

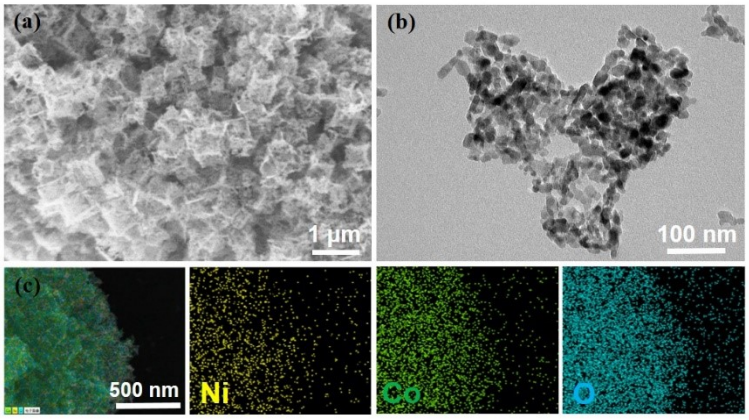

Fig S2. (a) SEM, (b) TEM, (c) SEM elemental mapping of $NiCo_2O_4$.

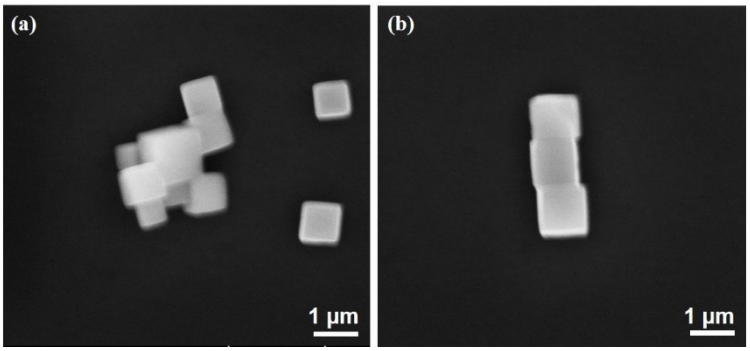

Fig S3. (a, b) SEM Images of ZIF-67.

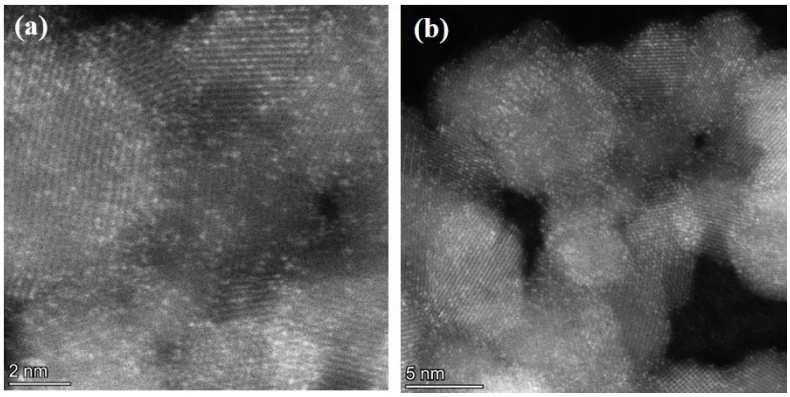

Fig. S4. (a, b) HAADF-STEM images of Ir_H-$NiCo_2O_4$ at different resolution, in which the bright spots are ascribed to Ir single atoms.

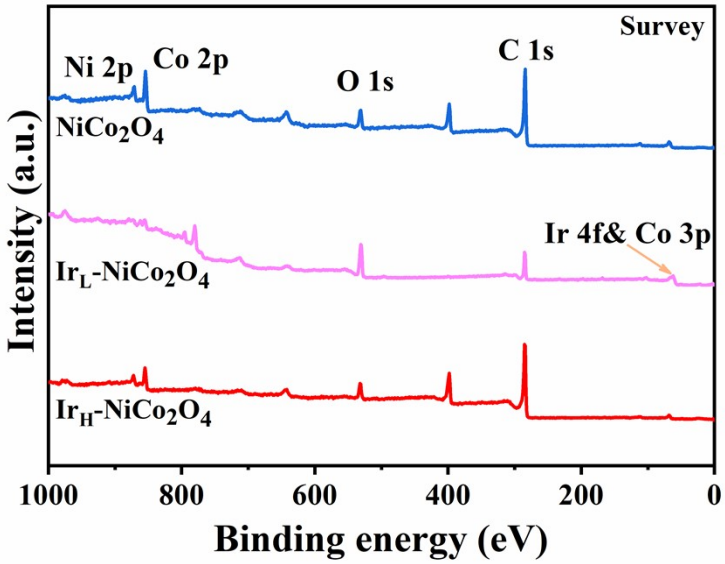

Fig. S5. XPS survey spectrums for pure $NiCo_2O_4$ (b) Ir_L-$NiCo_2O_4$ (c) Ir_H-$NiCo_2O_4$

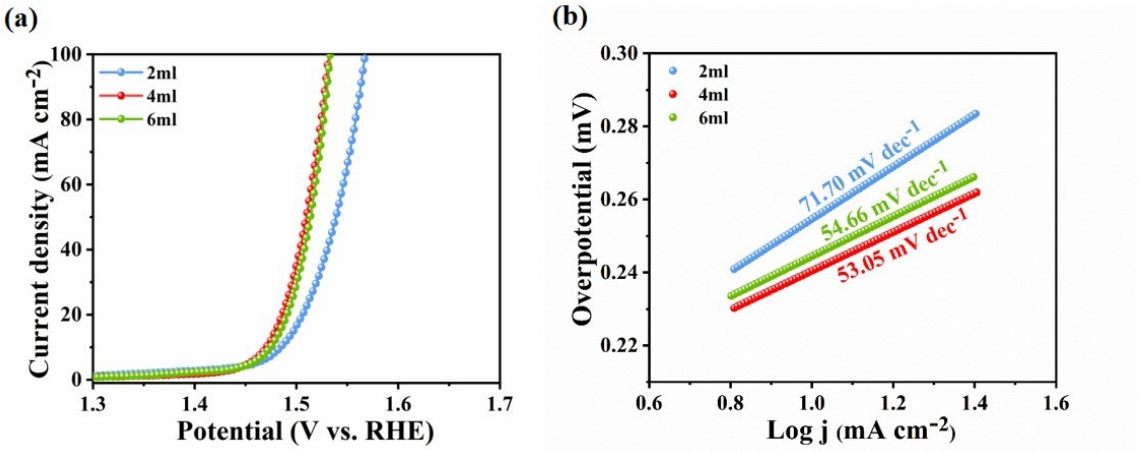

Fig S6. (a) LSV curves of Ir_H-$NiCo_2O_4$ fabricated with different content of Ir. (b) The corresponding Tafel plots.

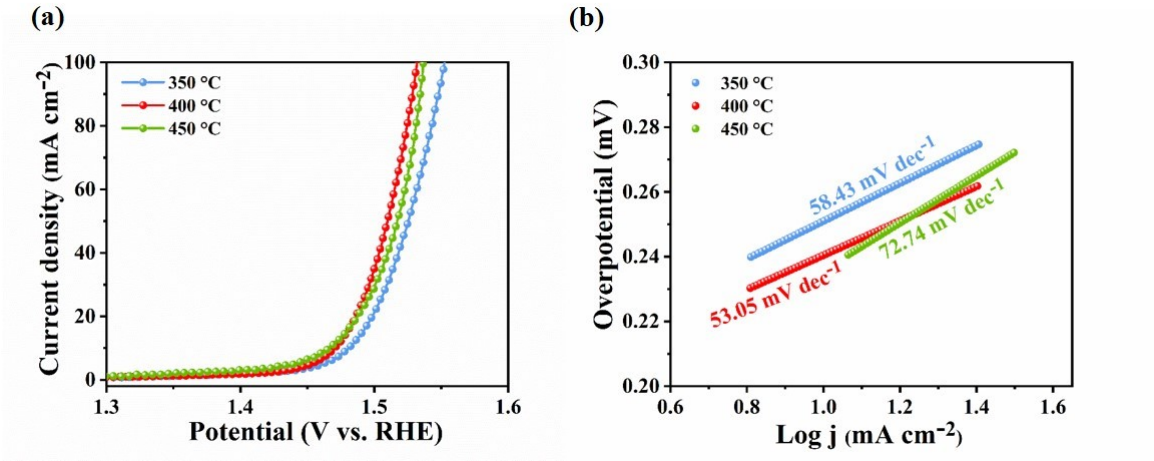

Fig S7. (a) LSV curves of Ir_H-$NiCo_2O_4$ fabricated with different reaction temprature. (b) The corresponding Tafel plots.

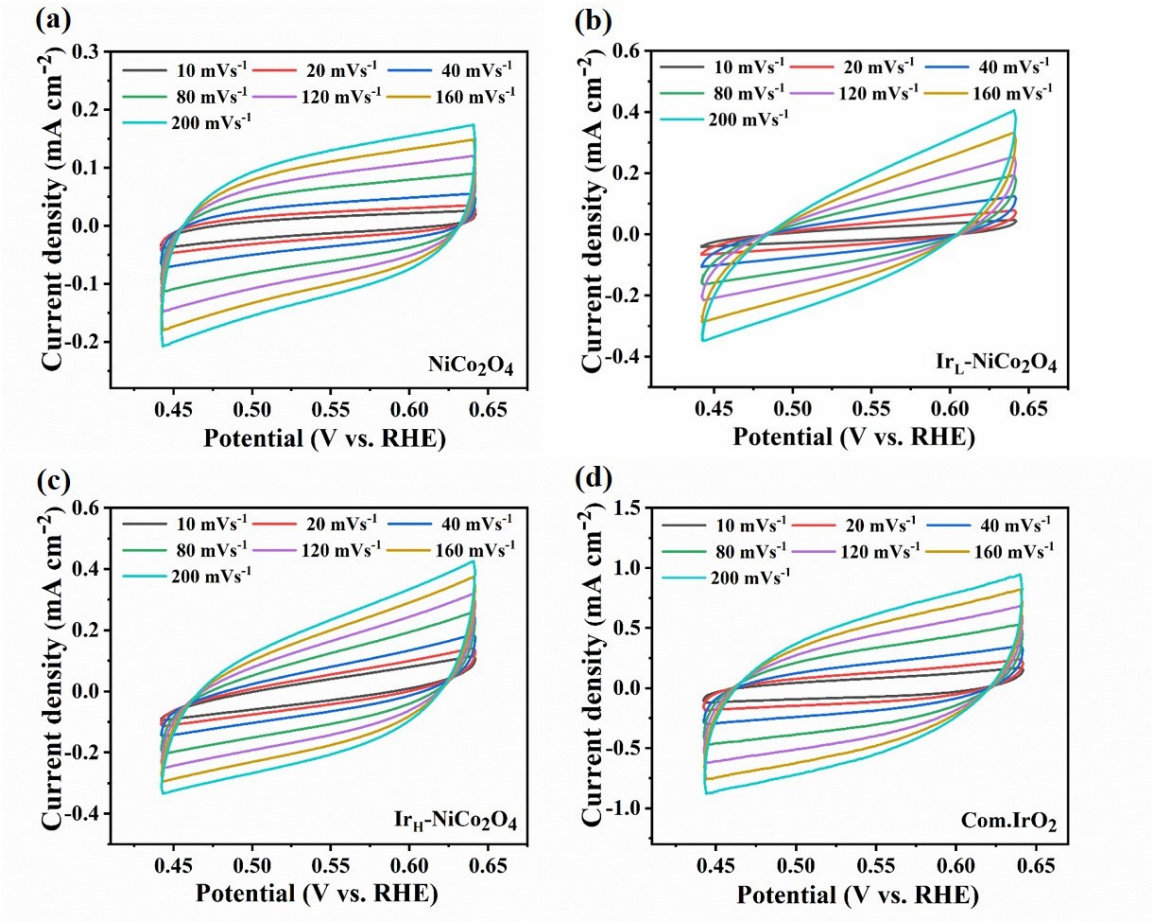

Fig S8. CVs measured for (a) pure $NiCo_2O_4$ (b) Ir_L-$NiCo_2O_4$ (c) Ir_H-$NiCo_2O_4$ and (d) Com. IrO_2 at different scan rates of 10, 20, 40, 80, 120, 160, and 200 mV s^{-1}.

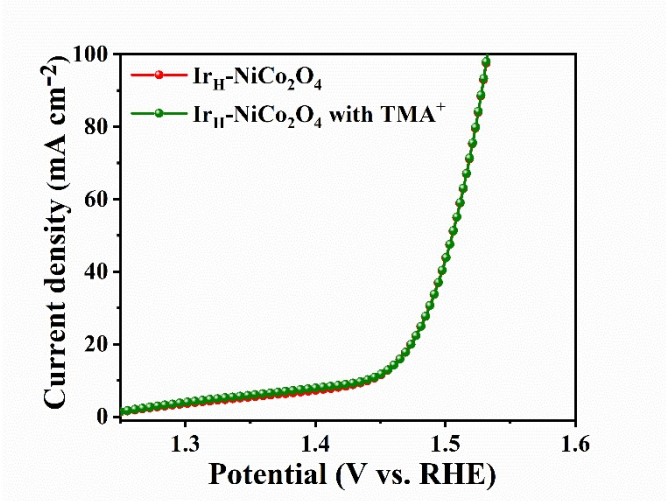

Figure S9. LSV curves of Ir_H-$NiCo_2O_4$ catalysts in 0.5 M H_2SO_4 electrolyte with or without TMA^+.

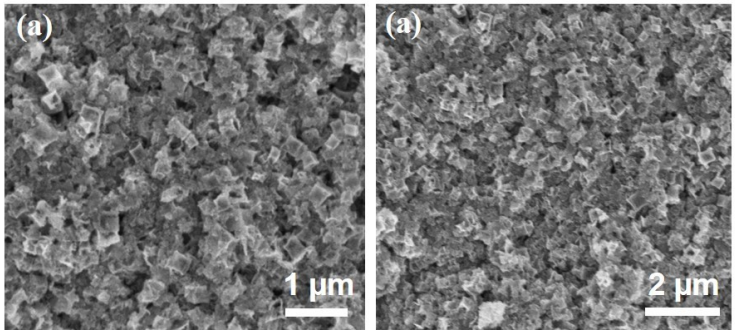

Fig S10. (a, b) SEM Images of Ir_H-$NiCo_2O_4$ at different resolution after the stability test.

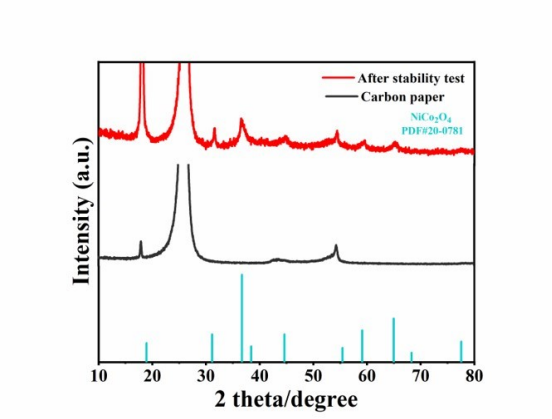

Fig S11. XRD of Ir_H-$NiCo_2O_4$ after the stability test.

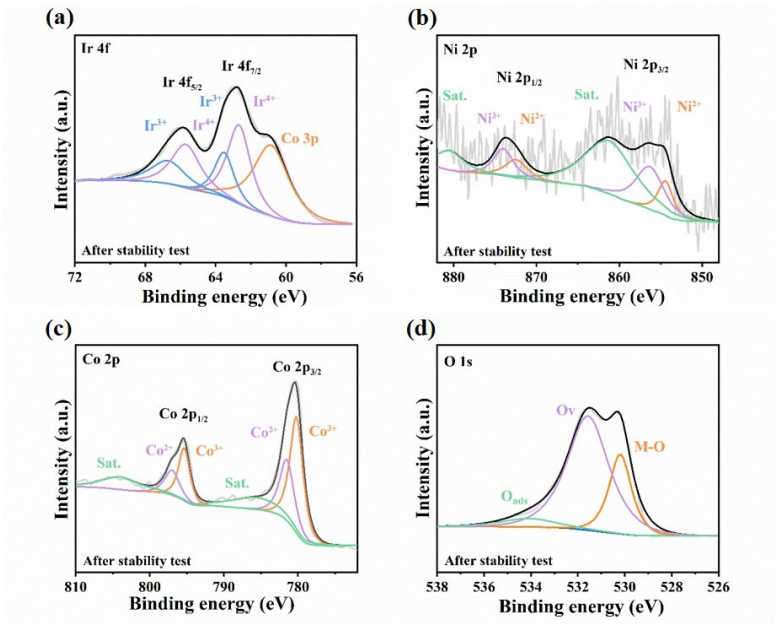

Fig. S12. High-resolution XPS spectra of (a) Ir 4f (b) Ni 2p (b) Co 2p and (c) O 1s XPS spectra of Ir_H-$NiCo_2O_4$ after the stability test.

Table 1. Ni and Co mass and atomic percent of pure $NiCo_2O_4$ by SEM-EDX.

Elements	**Ni**	**Co**	**O**
Mass Fraction %	22.94	49.37	27.69
Atomic Fraction%	13.20	28.31	58.49

Table S2. Ir, Ni and Co weight percent of pure $NiCo_2O_4$, Ir_L-$NiCo_2O_4$ and Ir_H-$NiCo_2O_4$ characterized by ICP-MS.

Sample	Element	Weight % (ICP-MS)
$NiCo_2O_4$	Ni Co	13.48 45.92
Ir_L-$NiCo_2O_4$	Ir Ni Co	3.66 11.23 40.72
Ir_H-$NiCo_2O_4$	Ir Ni Co	7.98 5.36 41.80

Table S3. The comparison of OER performance of our catalysts with previously reported catalysts in acidic electrolyte.

Catalyst	electrolyte	η_{10} (mV)	Stability (h)	Mass loading (mg/cm^2)	References
Ir_H-$NiCo_2O_4$	0.5 M H_2SO_4	240	282	0.25	This work
DNP-IrNi	0.5 M H_2SO_4	248	50	0.67	[1]
$Ir_{0.06}Co_{2.94}O_4$	0.1 M $HClO_4$	292	240	-	[2]
IrO_x/Zr_2ON_2	0.5 M H_2SO_4	255	5	0.38	[3]
Gd-$IrO_{2-\delta}$	0.5 M H_2SO_4	260	200	0.25	[4]
$W_{0.7}Ir_{0.3}O_y$	0.1 M $HClO_4$	278	55	0.25	[5]
IrCo-CoO	0.5 M H_2SO_4	270	140	0.15	[6]
UF-Ir/IrO_x	0.5 M H_2SO_4	299	200	-	[7]
Ir@WO_{3-x}	0.5 M H_2SO_4	276	110	0.10	[8]
Ti-IrO_x/Ir	0.5 M H_2SO_4	254	100	0.35	[9]
Ir_2Sm-S/G	0.5 M H_2SO_4	275	120	-	[10]

References:

1. K.-R. Yeo, K.-S. Lee, H. Kim, J. Lee and S.-K. Kim, A highly active and stable 3D dandelion spore-structured self-supporting Ir-based electrocatalyst for proton exchange membrane water electrolysis fabricated using structural reconstruction, *Energy & Environmental Science*, 2022, **15**, 3449-3461.
2. J. Shan, C. Ye, S. Chen, T. Sun, Y. Jiao, L. Liu, C. Zhu, L. Song, Y. Han and M. Jaroniec,Short-range ordered iridium single atoms integrated into cobalt oxide spinel structure for highly efficient electrocatalytic water oxidation, *Journal of the American Chemical Society*, 2021, **143**, 5201-5211.
3. C. Lee, K. Shin, Y. Park, Y. H. Yun, G. Doo, G. H. Jung, M. Kim, W. C. Cho, C. H. Kim and H. M. Lee, Catalyst-Support Interactions in Zr_2ON_2-Supported IrO_x Electrocatalysts to Break the Trade-Off Relationship Between the Activity and Stability in the Acidic Oxygen Evolution Reaction, *Advanced Functional Materials*, 2023, **33**, 2301557.
4. J. Wu, W. Zou, J. Zhang, L. Zhang, H. Song, Z. Cui and L. Du, Regulating Ir−O Covalency to Boost Acidic Oxygen Evolution Reaction, *Small*, 2024, **20**, 2308419.
5. T. Yan, S. Chen, W. Sun, Y. Liu, L. Pan, C. Shi, X. Zhang, Z.-F. Huang and J.-J. Zou, IrO_2 nanoparticle-decorated Ir-doped $W_{18}O_{49}$ nanowires with high mass specific OER activity for proton exchange membrane electrolysis, *ACS Applied Materials & Interfaces*, 2023, **15**, 6912-6922.
6. B. Zaman, J. Fan, D. Wang, H. Fan, M. Gong, M. Faizan and X. Cui, Surface-Segregated IrCo Nanoparticles on CoO Nanosheets with Ultralow Ir Loading for Efficient Acidic Water Splitting, *ChemCatChem*, 2024, **16**, e202400795.
7. A. Chen, M. Deng, Z. Lu, Y. Lin and L. Chen, Ultrafine iridium nanoparticles prepared without a surfactant for the acidic oxygen evolution reaction, *Materials Chemistry Frontiers*, 2023, **7**, 4900-4907.

8. X. Ma, C. Yang, F. Zhang, F. Ke, Q. Cheng, L. Zou and H. Yang, Oxygen-vacancy-rich tungsten oxide boosted ultrasmall iridium nanoparticles for acidic oxygen evolution, *International Journal of Hydrogen Energy*, 2023, **48**, 36776-36783.
9. Y. Wang, R. Ma, Z. Shi, H. Wu, S. Hou, Y. Wang, C. Liu, J. Ge, W. Xing. Inverse doping IrOx/Ti with weakened Ir-O interaction toward stable and efficient acidic oxygen evolution. *Chem*, **9**, (2023) 2931-2942.
10. S. Zhang, L. Yin, Q. Li, S. Wang, W. Wang and Y. Du, Laves phase Ir_2 Sm intermetallic nanoparticles as a highly active electrocatalyst for acidic oxygen evolution reaction, *Chemical Science*, 2023, **14**, 5887-5893.